

## LYMPHOID NEOPLASIA

A critical role of autocrine sonic hedgehog signaling in human CD138<sup>+</sup> myeloma cell survival and drug resistance

Zhiqiang Liu, Jingda Xu, Jin He, Yuhuan Zheng, Haiyan Li, Yong Lu, Jianfei Qian, Pei Lin, Donna M. Weber, Jing Yang, and Qing Yi

Department of Lymphoma and Myeloma, Division of Cancer Medicine, The University of Texas MD Anderson Cancer Center, Houston, TX.

## Key Points

- CD138<sup>+</sup> MM cells are a major source of SHH.
- Autocrine SHH enhances MM drug resistance.

Hedgehog (Hh) signaling plays an important role in the oncogenesis of B-cell malignancies such as multiple myeloma (MM). However, the source of Hh ligand sonic hedgehog (SHH) and its target cells remains controversial. Previous studies showed that stromally induced Hh signaling is essential for the tumor cells and that CD19<sup>+</sup>CD138<sup>-</sup> MM stem cells are the target cells of Hh signaling. Here we demonstrate that SHH was mainly secreted by human myeloma cells but not by stromal cells in MM bone marrow. Autocrine SHH enhanced CD138<sup>+</sup> myeloma cell proliferation and protected myeloma cells from

spontaneous and stress-induced apoptosis. More importantly, autocrine SHH protected myeloma cells against chemotherapy-induced apoptosis *in vitro* and *in vivo*. Combinational treatment with chemotherapy and SHH-neutralizing antibody displayed synergistic antimyeloma effects. Mechanistic studies showed that SHH signaling activated the SHH/GLI1/BCL-2 axis, leading to the inhibition of myeloma cell apoptosis. Thus, this study identifies the myeloma autocrine Hh signaling pathway as a potential target for the treatment of MM. Targeting this pathway may improve the efficacy of chemotherapy in MM patients. (*Blood*. 2014;124(13):2061-2071)

## Introduction

Multiple myeloma (MM) is largely incurable.<sup>1</sup> It accounts for approximately 1% of neoplastic diseases and 13% of hematologic malignancies.<sup>2</sup> In past decades, because of advancements in understanding the molecular pathogenesis of the disease and the availability of stem cell transplantation and new drugs, the overall survival rate of patients with MM has significantly increased. However, only up to 35% of patients with MM achieve 5-year relative survival after receiving current therapies, and patients are prone to quickly relapse and have refractory disease after high-dose chemotherapy.<sup>3</sup> Therefore, a better understanding of the mechanism underlying MM cell resistance to chemotherapy would be beneficial in the development of novel therapeutic approaches and would improve patient outcomes.

Hedgehog (Hh) signaling is essential for embryonic development and adult tissue homeostasis. Its components are highly conserved from *Drosophila* to vertebrates.<sup>4,5</sup> Three Hh ligands—sonic hedgehog (SHH), indian hedgehog (IHH), and desert hedgehog (DHH)—have been identified in mammals. Activation of Hh signaling is initiated by the binding of Hh ligands to the Hh receptor Patched (PTCH), and consequently the release of Smoothened (SMO), thereby leading to the activation of the transcription factors Gli1 and Gli2 and the upregulation of the expression of Gli target genes.<sup>6,7</sup>

Recently, aberrant activation of Hh signaling has been reported in solid tumors, such as basal cell carcinoma, medulloblastoma, and cancers of the pancreas, prostate, and lung,<sup>8</sup> and in hematologic malignancies, such as B-cell lymphoma and MM.<sup>9-11</sup> Some studies have suggested that Hh signaling activation may play an important role in the pathogenesis of tumors.<sup>12</sup> Dierks et al<sup>13</sup> reported that

stromally induced Hh signaling played an essentially role in B-cell malignancies, including lymphomas and myeloma, and Peacock et al<sup>14</sup> reported that Hh signaling is active only in CD138<sup>-</sup>CD19<sup>+</sup> MM stem cells but not in CD138<sup>+</sup>CD19<sup>-</sup> MM plasma cells. However, on the basis of our observation that Hh ligands, especially SHH, are highly expressed by bone marrow (BM) CD138<sup>+</sup> MM cells, we hypothesized that MM-derived autocrine SHH might be important in sustaining CD138<sup>+</sup> MM growth and survival. In this study, we demonstrated that MM cells, but not BM stromal cells, are the major producer and secretor of SHH and that autocrine SHH promotes the proliferation of and inhibits chemotherapy-induced apoptosis in CD138<sup>+</sup> MM cells *in vitro* and *in vivo*.

## Materials and methods

## Cells, transfection, and reagents

MM cell lines ARP-1, ARK, CAG, MM.1S, RPMI-8226, and U266 have been described previously.<sup>15</sup> Primary MM cells from BM aspirates of MM patients were isolated by using anti-CD138 antibody-coated magnetic beads (Miltenyi Biotec). The study was approved by the institutional review board at The University of Texas MD Anderson Cancer Center and was conducted in accordance with the Declaration of Helsinki.

For transient transfections of HEK293 cells and CAG cells, Lipofectamine 2000 (Invitrogen) was used, and for ARP-1 cells, the Neon transfection system (Invitrogen) was used. Stable cell line screening was performed with 800 μg/mL of neomycin (Sigma-Aldrich) for 4 weeks, and positive cells were selected for the *in vivo* studies.

Submitted March 12, 2014; accepted June 30, 2014. Prepublished online as *Blood* First Edition paper, July 21, 2014; DOI 10.1182/blood-2014-03-557298.

The online version of this article contains a data supplement.

There is an Inside *Blood* Commentary on this article in this issue.

The publication costs of this article were defrayed in part by page charge payment. Therefore, and solely to indicate this fact, this article is hereby marked "advertisement" in accordance with 18 USC section 1734.

© 2014 by The American Society of Hematology

### Real-time polymerase chain reaction and western blotting

Total RNA was isolated by using an RNeasy kit (Qiagen). The total RNA (1  $\mu$ g) was subjected to reverse transcription by using a SuperScript II (Invitrogen) reverse transcription-polymerase chain reaction (RT-PCR) kit; 1  $\mu$ L of the final complementary DNA was applied to real-time PCR amplification with SYBRGreen by using a StepOnePlus real-time PCR system (Applied Biosciences).

Western blotting was carried out as previously described.<sup>16</sup> Briefly, cells were lysed, and 50  $\mu$ g of total protein was separated via electrophoresis on a 4% to 12% gel (Invitrogen). The gel was then transferred onto a nitrocellulose membrane, immunohybridized with primary antibodies at 4°C overnight, and incubated with second antibodies at room temperature for 1 hour. After wash, the immunoblot was developed by using a chemiluminescence substrate (Thermo Scientific).

### Cell proliferation, apoptosis, and luciferase assay

MM cells were incubated with different reagents for different times (1 to 5 days), then incubated for 1 hour with a cell proliferation assay kit solution (Promega), and finally measured at a 490 nm wavelength. An apoptosis assay was performed as previously described.<sup>17</sup> HEK293 cells were transfected with 0.9  $\mu$ g of 8 $\times$  Gli-BS Luc plasmid and 0.1  $\mu$ g of pRL-TKRenilla plasmid (Promega) using Lipofectamine 2000 (Invitrogen) for 24 hours, and the cell lysate was used to detect luciferase activity in a Dual-Luciferase Reporter assay system (Promega).

### Immunohistochemistry

Paraffin-embedded sections were deparaffinized and blocked, incubated with 1:200 anti-SHH antibody (Millipore) at 4°C overnight, and then incubated with horseradish peroxidase-conjugated secondary antibody at 1:500 for 1 hour at room temperature. The sections were developed by using a DAB substrate kit (Thermo Scientific) at room temperature for 1 to 5 minutes and then counterstained with hematoxylin.

### Animal studies

CB.17 SCID mice were used, and the studies were approved by the Institutional Animal Care and Use Committee at MD Anderson Cancer Center. Ten (per group) 6- to 8-week-old female mice were subcutaneously inoculated in the right flank with  $2 \times 10^6$  MM cells. The SCID-hu mouse model was established as previously described.<sup>18</sup> Tumor volume (in cubic millimeters) was measured every 3 days in two dimensions by using a caliper and was calculated as  $0.4 \times (\text{short length})^2 \times \text{long length}$ . Sera were collected every 6 days from the mice during treatment and tested for MM-secreted M-proteins or their light chains by using an enzyme-linked immunosorbent assay. Mice were humanely euthanized when they became moribund or when the subcutaneous tumors reached 15 mm in diameter.

### Statistical analysis

Experimental values are expressed as mean  $\pm$  standard error of the mean if not otherwise indicated. Statistical significance was analyzed by using SPSS 10.0 software and was determined by unpaired Student *t* tests and one-way analysis of variance. A *P* value  $< .05$  was considered statistically significant. All results were reproduced in at least 3 independent experiments.

## Results

### MM cells, but not BM microenvironment cells, predominantly express and secrete SHH

To examine the role of autocrine versus paracrine SHH in myeloma cell growth and survival, the first question we asked was which type of cell, myeloma or stromal, was the major contributor of SHH in the BM of MM patients. First, we analyzed the gene expression patterns of SHH in MM cells in the public databases<sup>19</sup> by using cancer outlier profile analysis for 258 MM patients in Walker's database, 247 MM

patients in Dickens' database, and 173 MM patients in Tian's database. We found that SHH messenger RNA (mRNA) was commonly expressed by purified CD138<sup>+</sup> primary MM cells (supplemental Figure 1A-C; see supplemental Data, available at the *Blood* Web site).

Second, we examined SHH protein expression in BM biopsy samples from patients with MM and healthy donors. Compared with normal BM (Figure 1Aa), high SHH protein levels were detected in the BM samples of all 5 MM patients examined (Figure 1Ab,c,e-g). More importantly, only myeloma plasma cells, but not non-plasma cells, in the MM BM samples expressed SHH (Figure 1Ad,h and higher magnification fields from Figure 1Ac,g, respectively). By counting SHH-positive cells, we found that up to 90% of MM plasma cells were SHH positive in the MM BM samples, whereas very few SHH-positive cells could be detected in normal BM samples or in non-plasma cells in MM BM samples (Figure 1B). Although a previous study showed that cultured BM stromal cells (most likely mesenchymal stromal cells [MSCs]) produced a large amount of SHH and could provide paracrine SHH to MM cells, the frequency of MSCs (Figure 1C, upper panels) detected by expression of CD90 and CD166<sup>20,21</sup> in MM BM (Figure 1C; middle panels) or normal BM (Figure 1C, lower panels) samples was extremely low.

Third, to confirm that CD138<sup>+</sup> MM plasma cells are the main producer of SHH and also to examine whether CD138<sup>+</sup> plasma cells or CD138<sup>-</sup>CD19<sup>+</sup> MM stem cells<sup>14</sup> manifest the Hh pathway activity, we isolated cells from MM patients' BM aspirates, stained the cells with CD138, CD19, and SHH antibodies, and selected the CD138<sup>-</sup>CD19<sup>-</sup> (non-plasma cells), CD138<sup>-</sup>CD19<sup>+</sup> (MM stem cells or B cells), and CD138<sup>+</sup>CD19<sup>-</sup> (MM plasma cells) populations for analysis of SHH expression by flow cytometry (Figure 2A). As shown in Figure 2B, more than 90% of CD138<sup>+</sup>CD19<sup>-</sup> plasma cells expressed SHH, but only very few CD138<sup>-</sup>CD19<sup>+</sup> MM stem cells or B cells or CD138<sup>-</sup>CD19<sup>-</sup> non-plasma cells expressed SHH. We next examined the mRNA levels of Hh ligands *SHH*, *DHH*, and *IHH*; Hh signaling receptor *PTCH1*; and transcription factor *GLI1* in primary MM cells and established MM cell lines by using RT-PCR and real-time PCR. All primary MM cells and cell lines expressed high levels of hedgehog receptor *PTCH1* and the key transcriptional factor *GLI1*, although the levels varied in different samples (Figure 2C). *SHH* expression was the highest and most consistent in all examined CD138<sup>+</sup> primary MM cells and MM cell lines. As analyzed by quantitative PCR, the average *SHH* expression was 30-fold higher than that of purified CD138<sup>-</sup>CD19<sup>+</sup> MM stem cells or B cells from MM patients' BM aspirates, but *IHH* and *DHH* were only slightly increased (Figure 2D). Using western blot analysis, we confirmed that SHH, PTCH, and GLI1 proteins were expressed in all examined MM cell lines, although their levels varied among different MM cells (Figure 2E).

Finally, we detected the expression of dispatched (DISP) receptors by the cells, because Hh ligand secretion from vertebrate cells is accomplished via two events: cholesterol modification of the N terminus and binding to the membrane protein DISP.<sup>22</sup> Our RT-PCR results for CD138<sup>+</sup> primary MM cells and MM cell lines indicated that SHH secretion was *DISP1* dependent, because the expression of both *DISP1* and *DISP2* was dominant in all of these samples (Figure 3A). In line with these findings, high levels of soluble SHH were detected in the 12-hour culture supernatants of CD138<sup>+</sup> primary MM cells and MM cell lines but not in those of purified CD138<sup>-</sup>CD19<sup>+</sup> cells from MM patients' BM aspirates (Figure 3B). Taken together, these results clearly showed that CD138<sup>+</sup> MM plasma cells, but not BM stromal cells, are the major producer of SHH protein and that CD138<sup>+</sup> plasma cells process Hh signaling components.

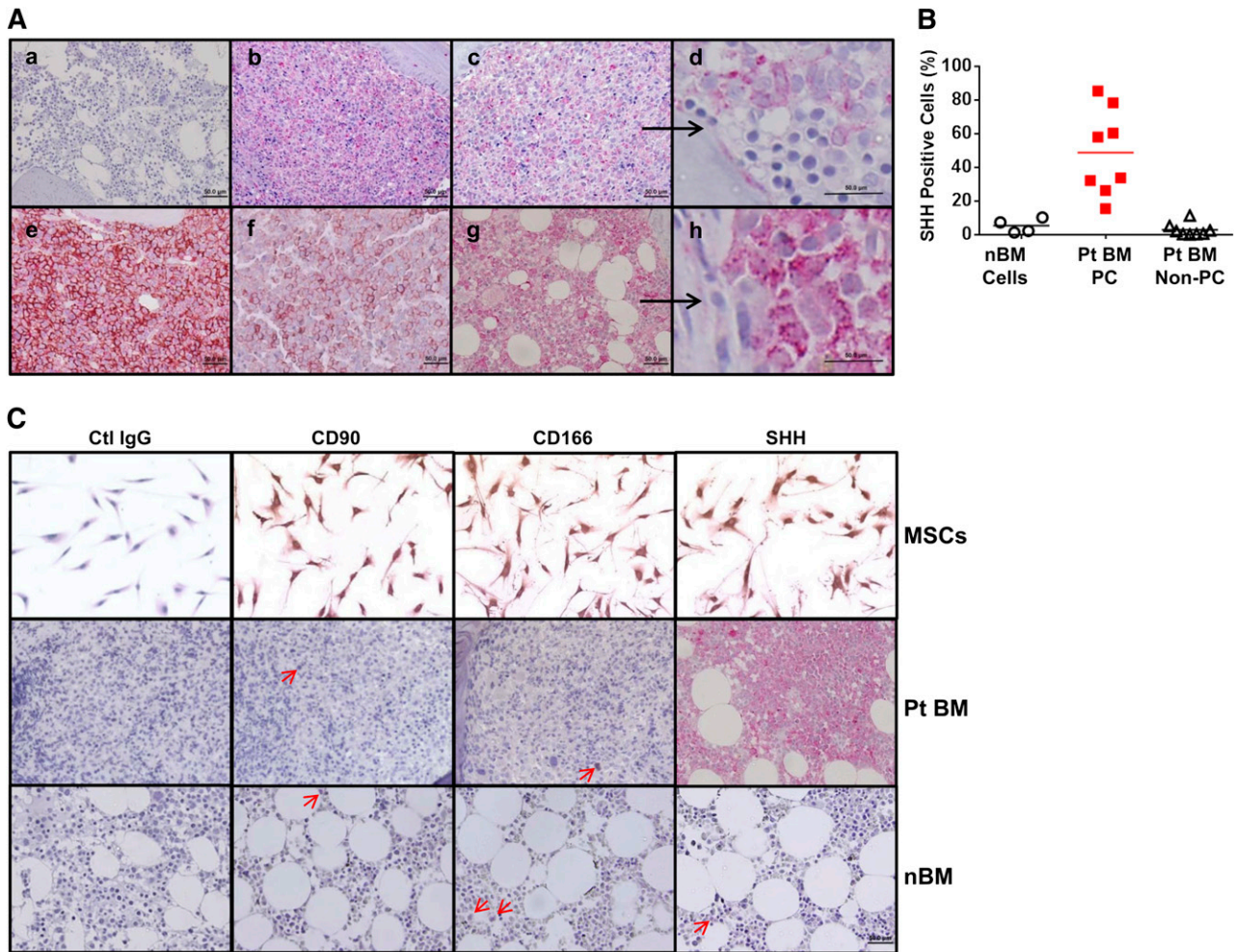


**Figure 1. Expression of SHH in BM biopsy samples from MM patients and healthy donors.** (A) Immunohistochemistry staining for SHH in BM samples of (a) 1 of 4 healthy donors or (b,c,e,f,g) 1 of 5 MM patients. Higher magnifications—in (d), they were derived from the (c) field (black arrow) or in (h), they were derived from the (g) field (black arrow)—show that SHH staining was observed only in MM plasma cells but not in non-plasma cells or BM hematopoietic cells. (B) Percentages of SHH-positive cells in normal BM (nBM cells) from 4 healthy donors and SHH-positive MM plasma cells (Pt BM PC) or MM non-plasma cells (Pt BM non-PC) from 8 MM patients (Pts). (C) Morphology and staining for CD90, CD166, and SHH in cultured MSCs (upper panels), MM patients' BM samples (Pt BM; middle panels), and normal BM samples from healthy donors (lower panels). Only very few CD90<sup>+</sup> or CD166<sup>+</sup> MSCs or SHH-expressing cells (indicated by red arrows) could be detected in patient BM or normal BM. Ctrl, control.

**MM-derived SHH activates the Hh signaling pathway in MM cells**

To examine the effects of MM cell-derived SHH on MM cells, we manipulated MM cell lines to secrete more or less SHH by using genetic alterations. ARP-1 and CAG cells were transfected with an SHH overexpression plasmid (pBS-hSHH; <sup>SHH+</sup>ARP-1 or <sup>SHH+</sup>CAG), SHH-specific short hairpin RNAs (<sup>SHH-</sup>ARP-1 or <sup>SHH-</sup>CAG), or control vector (<sup>vec</sup>ARP-1 or <sup>vec</sup>CAG). Compared with the wild-type or control vector cells, <sup>SHH+</sup>ARP-1 and <sup>SHH+</sup>CAG cells expressed very high levels of SHH mRNA ( $P < .01$ ; supplemental Figure 2A-B), total protein (supplemental Figure 2C), and soluble protein ( $P < .01$ ; supplemental Figure 2D), whereas <sup>SHH-</sup>ARP-1 and <sup>SHH-</sup>CAG cells expressed low levels of mRNA and proteins ( $P < .01$ ). To determine whether MM-derived SHH could activate the Hh signaling pathway in MM cells, a Gli-luciferase reporter system<sup>23</sup> was used. HEK293 cells were transfected with control vector or Gli-luciferase reporter plasmids and then cocultured with or without ARP-1 or CAG cells that expressed and secreted SHH. In the cocultures, HEK293 cells were seeded on the bottom of wells, and ARP-1 or CAG cells were seeded in the Transwell inserts. For the supernatant setting, 12-hour culture media of wild-type,

SHH-overexpression, SHH-knockdown ARP-1 or CAG cells was added into HEK293 cells with a 1:1 dilution of fresh media. As shown in Figure 3C, Gli-luciferase activity was enhanced in HEK293 cells added with the supernatant of, or cocultured with <sup>SHH+</sup>ARP-1 cells, but not with <sup>vec</sup>ARP-1 cells ( $P < .05$ ), which demonstrates the ability of MM-derived SHH to activate the Hh signaling pathway. The addition of SHH-neutralizing antibody, but not control immunoglobulin G (IgG), significantly downregulated Gli-luciferase activity in HEK293 cells cocultured with <sup>SHH+</sup>ARP-1 cells ( $P < .01$ ), thereby confirming that MM-derived SHH mediated the effects. Similar results were also derived with <sup>SHH+</sup>CAG cells (Figure 3D). In addition, silencing the SHH gene could also downregulate Gli-luciferase activity, confirming the autocrine induction of Gli-luciferase activity in ARP-1 and CAG MM cells (Figure 3G). Moreover, addition of cyclopamine, an SMO-specific inhibitor,<sup>24</sup> or SHH-neutralizing antibody, but not dimethylsulfoxide (DMSO) or control IgG, also significantly downregulated the mRNA levels of *GLI1* and *PTCH1* in HEK293 cells cocultured with <sup>SHH+</sup>ARP-1 cells (Figure 3E). Similar results were also obtained from CAG cells (Figure 3F). To examine whether SHH expression was DISP-dependent, we knocked down DISP1, which is a dominant



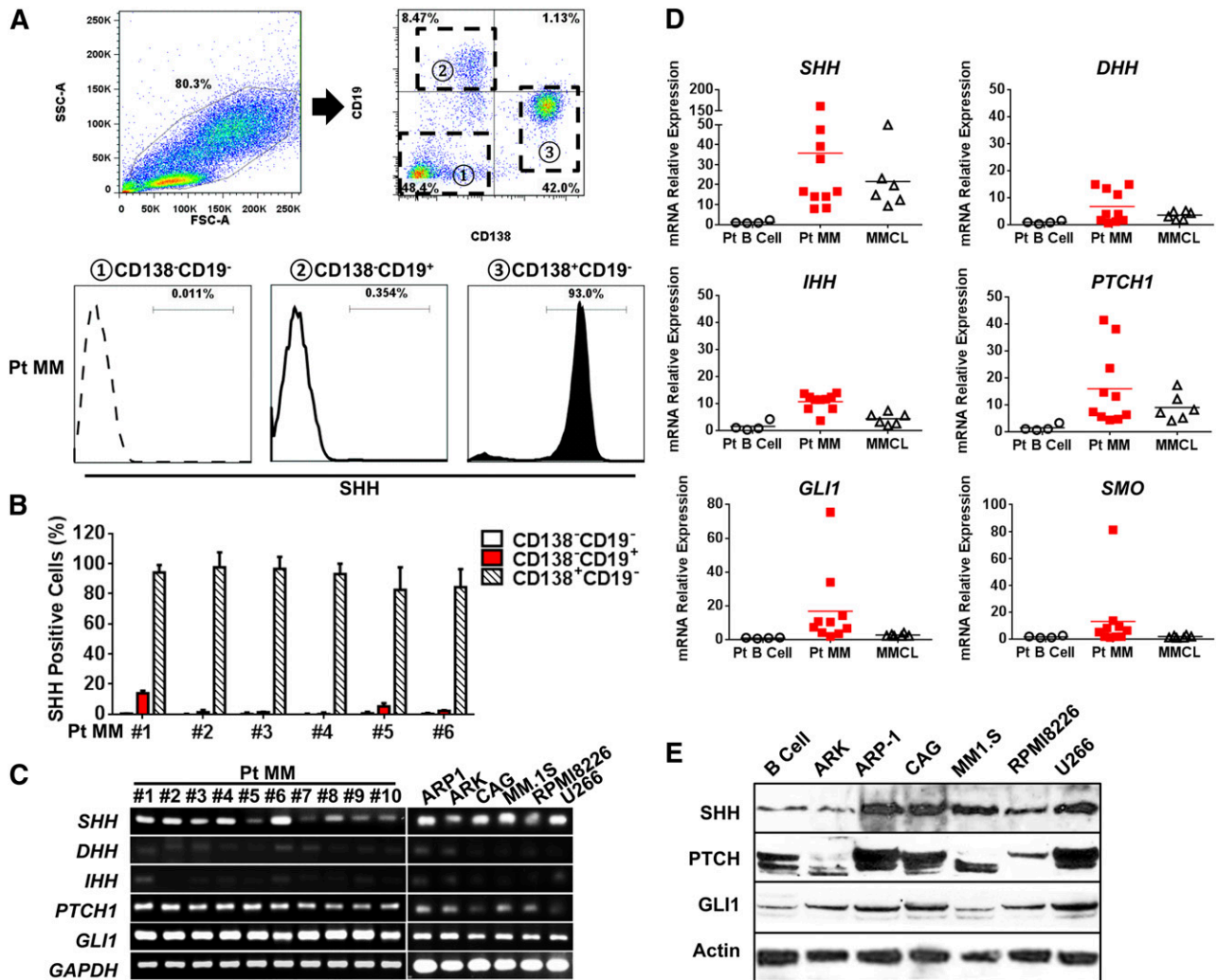


**Figure 2. Expression of SHH and Hh signaling pathway components in MM cells.** (A) Flow cytometry analysis for identification and selection of CD138<sup>-</sup>CD19<sup>-</sup>, CD138<sup>+</sup>CD19<sup>+</sup>, and CD138<sup>+</sup>CD19<sup>-</sup> cell populations from MM patients' BM aspirates for expression of SHH. (B) Percentages of SHH-positive cells in each of the 3 cell populations in BM samples from 6 more MM patients. (C) RT-PCR showing the levels of mRNA for Hh signaling components in highly purified CD138<sup>+</sup> primary MM cells from 10 MM patients (Pt MM) and 6 MM cell lines (MMCLs). (D) Real-time PCR showing the levels of mRNA for Hh signaling components in patients' highly purified CD19<sup>+</sup> B cells (Pt B cell; n = 4) or CD138<sup>+</sup> primary MM cells (Pt MM; n = 10) from MM patients' BM aspirates, and 6 MMCLs. (E) Western blotting showing protein expression of SHH, PTCH, GLI1, in MMCLs and purified CD19<sup>+</sup> B cells from healthy donor. GAPDH, glyceraldehyde phosphate dehydrogenase.

receptor of SHH in ARP-1 and CAG cells. We observed that the levels of SHH secretion were significantly reduced in DISP1-knockdown ARP-1 or CAG cells as compared with those in control cells ( $P < .001$ ; Figure 3H). Taken together, these results strongly suggest that the Hh signaling pathway is activated in MM cells and that SHH is a dominant Hh ligand secreted by MM cells with high biological activity.

#### MM-derived SHH promotes MM cell proliferation

To determine whether MM cell-secreted SHH has a biological function in MM cell proliferation, we tested the spontaneous proliferation of ARP-1 or CAG cells in normal culture media in the presence or absence of Hh signaling receptor antagonist or SHH-neutralizing antibody. After treating ARP-1 and CAG cells with cyclopamine for 3 days, the proliferation of ARP-1 and CAG cells was significantly inhibited ( $P < .01$  compared with DMSO control; Figure 4A). The addition of anti-SHH antibody, but not control IgG, decreased the proliferation of ARP-1 and CAG cells ( $P < .01$  compared with control IgG; Figure 4A). In addition, compared with <sup>vec</sup>ARP-1 cells, <sup>SHH+</sup>ARP-1 cells had a higher rate of

proliferation, whereas <sup>SHH-</sup>ARP-1 cells had a lower rate of proliferation ( $P < .01$ ; Figure 4B), and the same results were achieved in the <sup>SHH+</sup>CAG and <sup>SHH-</sup>CAG cells (Figure 4B). Similarly, the addition of recombinant human SHH (rhSHH) significantly enhanced, in a dose-dependent manner, the proliferation of ARP-1, CAG, RPMI-8226, and U266 cells (Figure 4C), and the addition of rhSHH to the culture of <sup>SHH-</sup>ARP-1 and <sup>SHH-</sup>CAG cells rescued the cell proliferation (supplemental Figure 3A-B). In contrast, treatment with anti-SHH antibody, but not control IgG, significantly downregulated, in a dose-dependent manner, the proliferation of ARP-1 and CAG cells ( $P < .01$ ; supplemental Figure 4A-B). These results indicate that MM cell-produced SHH enhances MM cell proliferation in an autocrine fashion.

#### MM-derived SHH reduces spontaneous apoptosis of MM cells

To determine whether MM-derived SHH affects MM cell apoptosis, we cocultured primary CD138<sup>+</sup> MM cells with rhSHH or SHH-neutralizing antibody. The addition of rhSHH decreased, in a dose-dependent manner, the percentage of apoptotic primary MM cells in

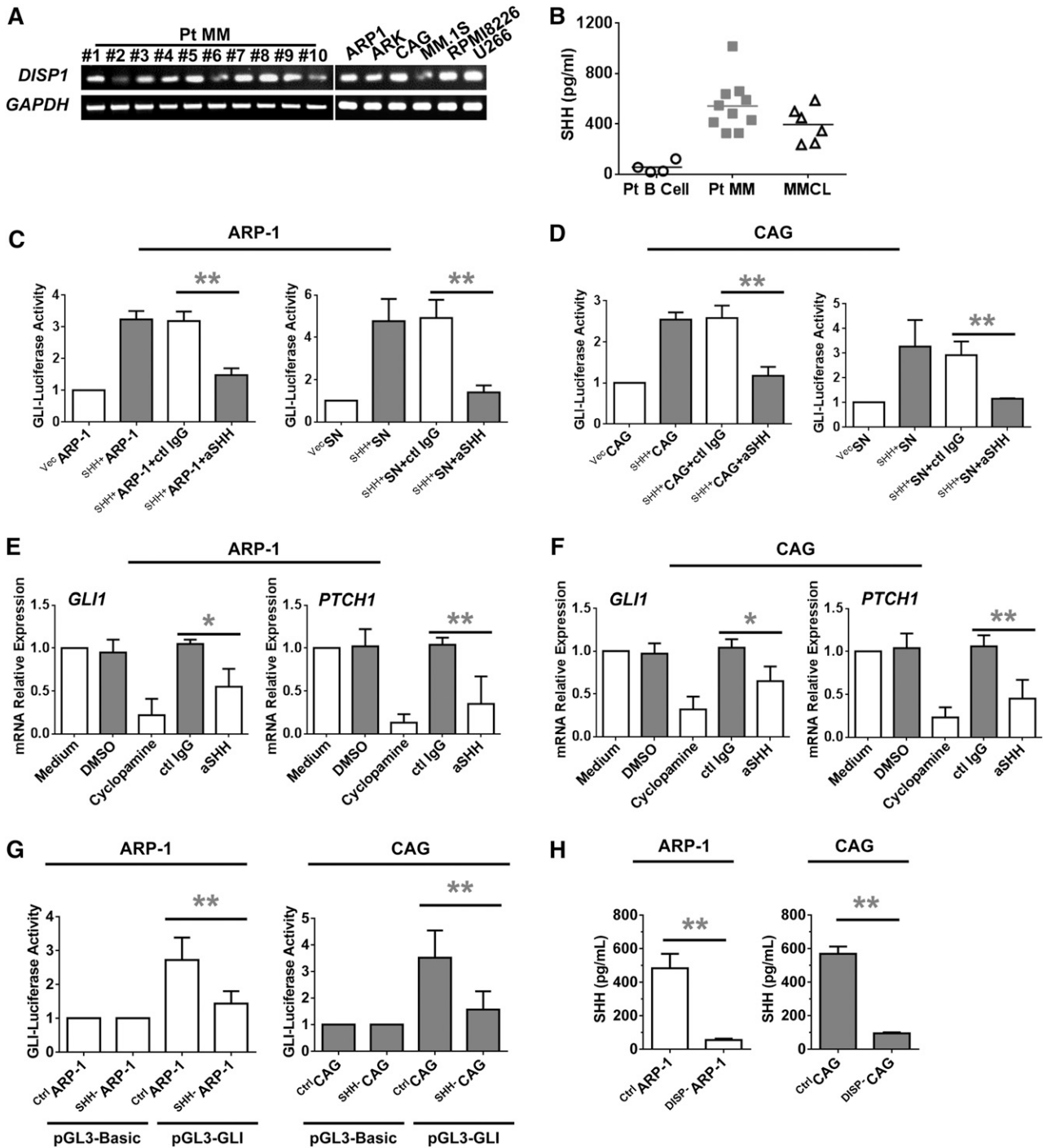


**Figure 3. Secretion and functional activity of MM-derived SHH.** (A) RT-PCR showing the levels of mRNA for *DISP1* in highly purified CD138<sup>+</sup> primary MM cells from 10 patients with MM (Pt MM) and 6 MMCLs. (B) Enzyme-linked immunosorbent assay (ELISA) showing the levels of secreted SHH in culture media of highly purified CD19<sup>+</sup> B cells (Pt B cell; n = 4) or CD138<sup>+</sup> primary MM cells (Pt MM; n = 10) from MM patients' BM aspirates and 6 MMCLs. (C-D) Hh signaling detected as luciferase activity in HEK293 cells induced by coculture with MM cells (left panels) or culture with MM cell culture supernatants (SNs; right panels). (E-F) Hh signaling detected as levels of mRNA examined by real-time PCR for *GLI1* (left panels) and *PTCH1* (right panels) in MM cells induced by MM-derived SHH in the presence or absence of cyclopamine (10  $\mu$ M) or SHH-neutralizing antibody (aSHH; 5  $\mu$ g/mL) for 48 hours. (G) Luciferase reporter gene assay shows the reduced pGL3-GLI activity in SHH<sup>+</sup>-ARP-1 or SHH<sup>+</sup>-CAG cells. (H) ELISA shows the reduced SHH secretion in the supernatant of 24-hour cultured DISP1<sup>-</sup>-ARP-1 or DISP1<sup>-</sup>-CAG cells. \**P* < .05; \*\**P* < .01. ctrl, control.

all 6 patient samples (*P* < .01; Figure 4D) and in the primary MM cells from 3 other patients (*P* < .01; supplemental Figure 4C). On the contrary, the addition of SHH-neutralizing antibody, but not control IgG, to the cultures of primary MM cells increased the percentage of apoptotic cells (*P* < .01; Figure 4D and supplemental Figure 4D). Moreover, spontaneous apoptosis of primary MM cells was

significantly lower in cultures with SHH<sup>+</sup>-CAG cells than in cultures with vec<sup>-</sup>CAG cells or without CAG cells (*P* < .01; supplemental Figure 4E). These findings indicate that autocrine SHH signaling played a role in protecting the cells from undergoing spontaneous apoptosis.

We blocked SHH signaling to examine the effects on MM cell apoptosis. Treatment of MM cell lines with cyclopamine or

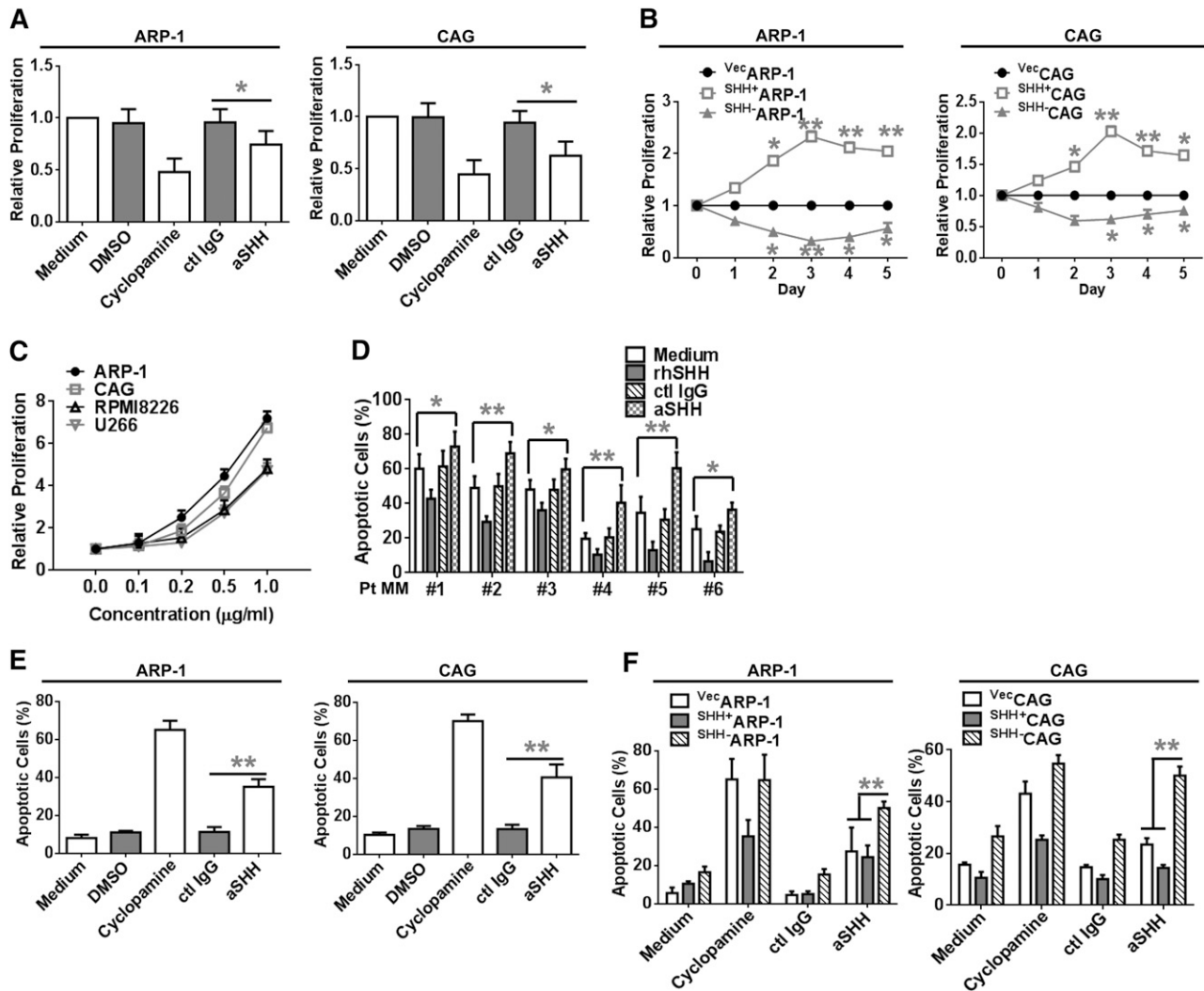


**Figure 4. MM-derived autocrine and exogenous SHH promote MM cell proliferation and survival.** Proliferation of (A) ARP-1 or CAG cells in culture media in the presence or absence of cyclopamine or aSHH. (B) Proliferation of <sup>vec</sup>ARP-1/CAG, <sup>SHH+</sup>ARP-1/CAG, or <sup>SHH-</sup>ARP-1/CAG cells in culture media. Cell proliferation was assayed daily for 5 consecutive days. (C) Proliferation of ARP-1, CAG, RPMI-8226, and U266 cells in culture media with the addition of different concentrations (0 to 1.0 μg/mL) of rhSHH. (D) Percentages of apoptotic CD138<sup>+</sup> primary MM cells purified from BM aspirates of 6 patients with MM (Pt MM) in a 24-hour culture with or without the addition of aSHH or control IgG (ctl IgG) (5 μg/mL) or rhSHH (5 ng/mL). (E) Percentages of apoptotic wild-type ARP-1 or CAG cells in a 3-day culture with or without the addition of cyclopamine (10 μM) or aSHH or control IgG (5 μg/mL). (F) Percentages of apoptotic <sup>vec</sup>ARP-1/CAG, <sup>SHH+</sup>ARP-1/CAG, or <sup>SHH-</sup>ARP-1/CAG cells in a 3-day culture with or without the addition of cyclopamine (10 μM) or aSHH or control IgG (5 μg/mL). Cell apoptosis was detected by Annexin-V binding assay. \**P* < .05; \*\**P* < .01.

anti-SHH antibody induced apoptosis in ARP-1 and CAG cells (Figure 4E). Treatment with DMSO or control IgG had no effect. In addition, spontaneous apoptosis was significantly lower in <sup>SHH+</sup>ARP-1 cells than in <sup>vec</sup>ARP-1 cells but much higher in <sup>SHH-</sup>ARP-1 cells treated with cyclopamine or SHH-neutralizing antibody (*P* < .01; Figure 4F). Similar results were obtained with CAG cells (*P* < .01; Figure 4F).

#### MM-derived SHH enhances MM cell chemotherapy resistance in vitro

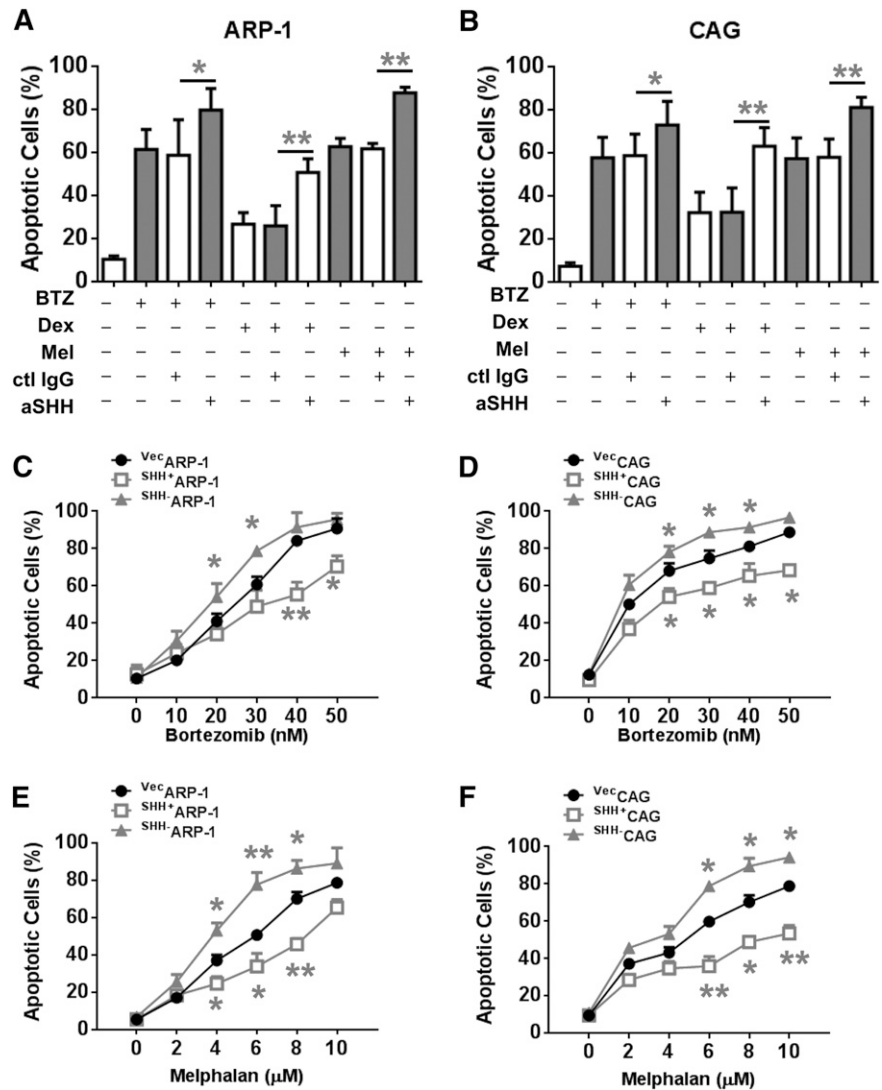
Next, we examined whether MM-derived SHH could protect MM cells from chemotherapy-induced apoptosis. We treated MM cells for 24 hours with dexamethasone, bortezomib (BTZ), and melphalan (Mel). Our results showed that BTZ at 10 nM, dexamethasone at 10 μM, and Mel at 5 μM induced apoptosis in about 50% of ARP-1 cells. The combination of BTZ or Mel and anti-SHH antibody increased the percentage of apoptotic ARP-1 cells to 70% to 80% (*P* < .01; Figure 5A). Similar results

were also found in CAG cells (Figure 5B). In contrast, the addition of rhSHH significantly reduced, in a dose-dependent manner, BTZ-induced apoptosis in ARP-1 and CAG cells (supplemental Figure 4F). Furthermore, compared with <sup>vec</sup>ARP-1 or <sup>vec</sup>CAG cells, <sup>SHH+</sup>ARP-1 or <sup>SHH+</sup>CAG cells were more resistant to treatment with BTZ (*P* < .01; Figure 5C-D) and Mel (*P* < .01; Figure 5E-F); however <sup>SHH-</sup>CAG or <sup>SHH-</sup>ARP-1 cells were more sensitive to treatment with BTZ and Mel (*P* < .01; Figure 5C-F). These findings strongly suggest that MM cell-produced SHH protects, in an autocrine fashion, MM cells from spontaneous and chemotherapy-induced apoptosis in vitro.

#### SHH inhibits MM cell apoptosis via activation of the SHH/GLI1/BCL-2 signaling pathway

We observed that treatment with BTZ upregulated the levels of cleaved caspase-9, caspase-3, and poly (ADP-ribose) polymerase (PARP) in MM cells (Figure 6A). The addition of rhSHH

**Figure 5. MM-derived autocrine and exogenous SHH induce MM-cell drug resistance.** Percentages of apoptotic (A) ARP-1 or (B) CAG cells induced by BTZ (10 nM), dexamethasone (Dex; 10  $\mu$ M), or Mel (5  $\mu$ M) in the presence or absence of aSHH or control IgG (5  $\mu$ g/mL). Also shown are percentages of apoptotic <sup>vec</sup>ARP-1/CAG, <sup>SHH+</sup>ARP-1/CAG, and <sup>SHH-</sup>ARP-1/CAG cells induced by different doses of (C,D) BTZ (0 to ~50 nM) or (E,F) Mel (0 to ~10  $\mu$ M). Apoptosis assay was performed for a 24-hour culture by using Annexin-V staining. \**P* < .05; \*\**P* < .01.



significantly reduced BTZ-induced activation and cleavage of caspase-9, caspase-3, and PARP in MM cells, whereas the addition of anti-SHH antibody upregulated BTZ-induced activation and cleavage of caspase-9, caspase-3, and PARP in MM cells (Figure 6A and supplemental Figure 5A). Similar results were also found in MM cells treated with Mel (Figure 6A and supplemental Figure 5A).

Because our results showed that the addition of SHH did not affect the expression of drug efflux transporters of the ATP binding cassette-containing family, such as TAP1, TAP2, MDR1, MDR2, and MDR3 (data not shown), we hypothesized that SHH may regulate the expression of BCL-2, a general antiapoptotic protein that inhibits the mitochondrial release of cytochrome C and downregulates caspase-9 cleavage.<sup>25</sup> In a dose-dependent manner, rhSHH upregulated and anti-SHH antibody downregulated the protein levels of BCL-2 and cleaved PARP in ARP-1 (Figure 6B and supplemental Figure 5B) treated with BTZ. We further showed that expression of BCL-2 and GLI1 was downregulated in the <sup>SHH-</sup>CAG cells and upregulated in the <sup>SHH+</sup>CAG cells compared with wild-type CAG cells (Figure 6C). To verify that SHH inhibited MM cell apoptosis via BCL-2, we used BCL-2 inhibitors HA 14-1 and ABT-737. Our results showed that BTZ or Mel induced MM cell apoptosis, whereas the addition of rhSHH reduced BTZ- or Mel-induced apoptosis of MM

cells (Figure 6D-E). However, the addition of HA 14-1 or ABT-737 (data not shown) partially restored BTZ-induced apoptosis in the cultures of MM cells in the presence of rhSHH (*P* < .01; Figure 6D-E). Taken together, these results strongly suggest that SHH activates GLI1 and upregulates the expression of BCL-2. SHH-mediated BCL-2 inhibits caspase-9-dependent cascade activation and apoptosis of MM cells.

**MM-derived SHH enhances MM cell growth and chemotherapy resistance in vivo**

To determine whether MM cell-produced SHH affects tumor growth and survival in vivo, we subcutaneously injected  $2 \times 10^6$  <sup>vec</sup>ARP-1, <sup>SHH+</sup>ARP-1, or <sup>SHH-</sup>ARP-1 cells into SCID mice. Twelve days after tumor cell injection, tumors were detectable in mice injected with <sup>vec</sup>ARP-1 cells. In comparison, palpable tumors were detected much earlier (at day 9) in mice injected with <sup>SHH+</sup>ARP-1 cells but much later (at day 18) in mice injected with <sup>SHH-</sup>ARP-1 cells (*P* < .01; Figure 7A). The tumor volumes were consistently larger and the M-protein levels were consistently higher in mice bearing <sup>SHH+</sup>ARP-1 tumors than in mice injected with <sup>vec</sup>ARP-1 cells (*P* < .01; Figure 7B). In contrast, tumor volumes were smaller and M-protein levels were lower in mice bearing <sup>SHH-</sup>ARP-1 cells than in mice injected

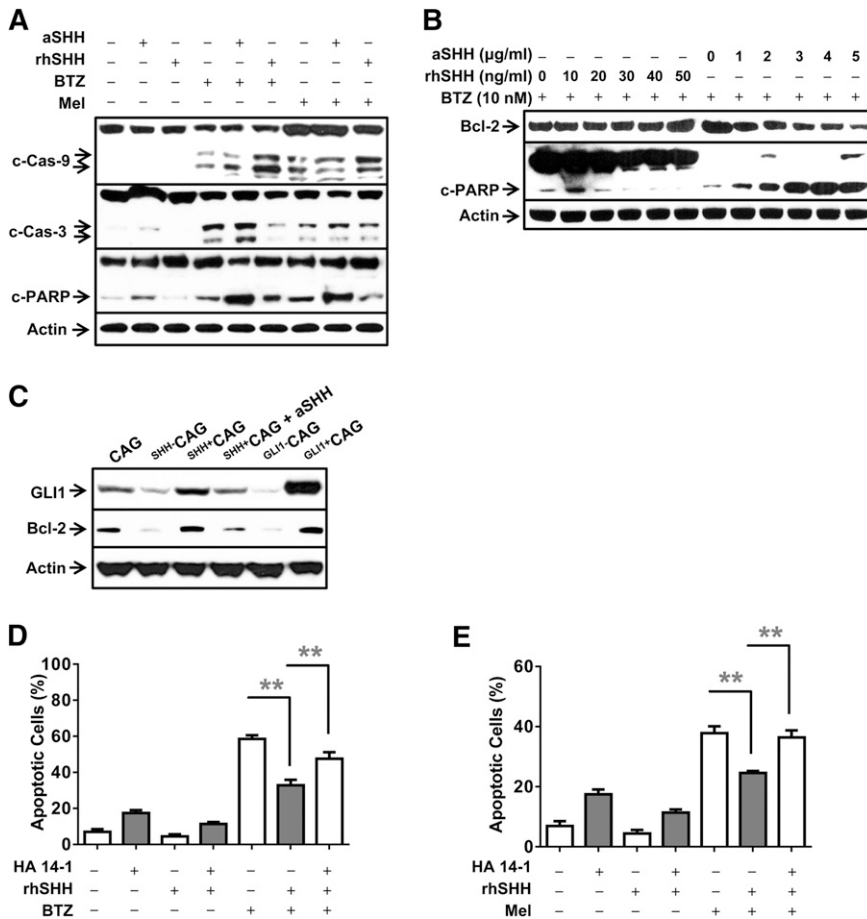


**Figure 6. Molecular mechanism of SHH-induced antiapoptotic signaling.** Western blot analysis showing protein levels of (A) caspases and cleaved (c-) caspases and PARP in MM (ARP-1) cells in 24-hour cultures with or without the addition of BTZ (10 nM) or Mel (5 μM) in the presence or absence of aSHH (5 μg/mL) or rhSHH (50 ng/mL). (B) BCL-2 and cleaved PARP (c-PARP) in MM (ARP-1) cells treated with BTZ (10 nM) in the presence of different concentrations of aSHH (0 to ~5 μg/mL) or rhSHH (0 to ~5 ng/mL) for 24 hours. (C) GLI1 and BCL-2 in CAG, SHH-CAG, SHH-CAG cells, or SHH-CAG cells in the presence of aSHH (5 μg/mL), and CAG cells transfected with 2 μg of pBSU6-GLI1 short hairpin RNA (GLI1-CAG) or pEGFP-GLI1 (GLI1-CAG) plasmid for 48 hours. Percentages of apoptotic ARP-1 cells treated with (D) BTZ (10 nM) or with (E) Mel (5 μM) without or with BCL-2 inhibitor HA 14-1 (20 μM) and/or rhSHH (50 ng/mL) for 24 hours. Cell apoptosis was examined by Annexin-V binding assay. \*\**P* < .01.

with <sup>vec</sup>ARP-1 cells (*P* < .01; Figure 7A-B). In line with this, the half survival time of <sup>vec</sup>ARP-1-bearing mice was 30 days, whereas the half survival time was 22 days for <sup>SHH</sup>ARP-1-bearing and 38 days for <sup>SHH</sup>-ARP-1-bearing mice (Figure 7C). Similar results were also obtained in mice injected with <sup>SHH</sup>+CAG or <sup>SHH</sup>-CAG cells (supplemental Figure 6A-B).

To examine the effects of SHH on the protection of MM cells from chemotherapy-induced apoptosis in vivo, we injected ARP-1-bearing mice with an intraperitoneal suboptimal dose of Mel (50 μg per mouse) or equal amounts of phosphate-buffered saline (PBS), anti-SHH antibody, or control IgG (around tumors) every 3 days. In addition, some Mel-treated mice were also injected with anti-SHH antibody or control IgG. Our results showed that treatment with Mel or anti-SHH antibody alone modestly reduced tumor volumes (*P* < .01; Figure 7D) and prolonged survival (Figure 7E) in the mice. However, the combination of anti-SHH antibody and Mel had synergistic anti-MM effects in terms of reducing tumor volumes (*P* < .01; Figure 7D). All the mice in the group treated with the combination of anti-SHH antibody and Mel survived during the observation period (Figure 7E). Immunohistochemical staining confirmed the expression of SHH in subcutaneous tumors from SCID mice injected with <sup>vec</sup>ARP-1, <sup>SHH</sup>+ARP-1, or <sup>SHH</sup>-ARP-1 cells (supplemental Figure 6C). Taken together, these results suggest that MM cell-produced SHH enhances tumor growth and survival and protects MM cells from chemotherapy in vivo.

Finally we performed an experiment to dissect the importance of the paracrine vs autocrine SHH on human MM growth and survival in vivo in the MM-SCID-hu mouse model.<sup>18,26,27</sup> We implanted human fetal bones that contained human BM into the flanks of

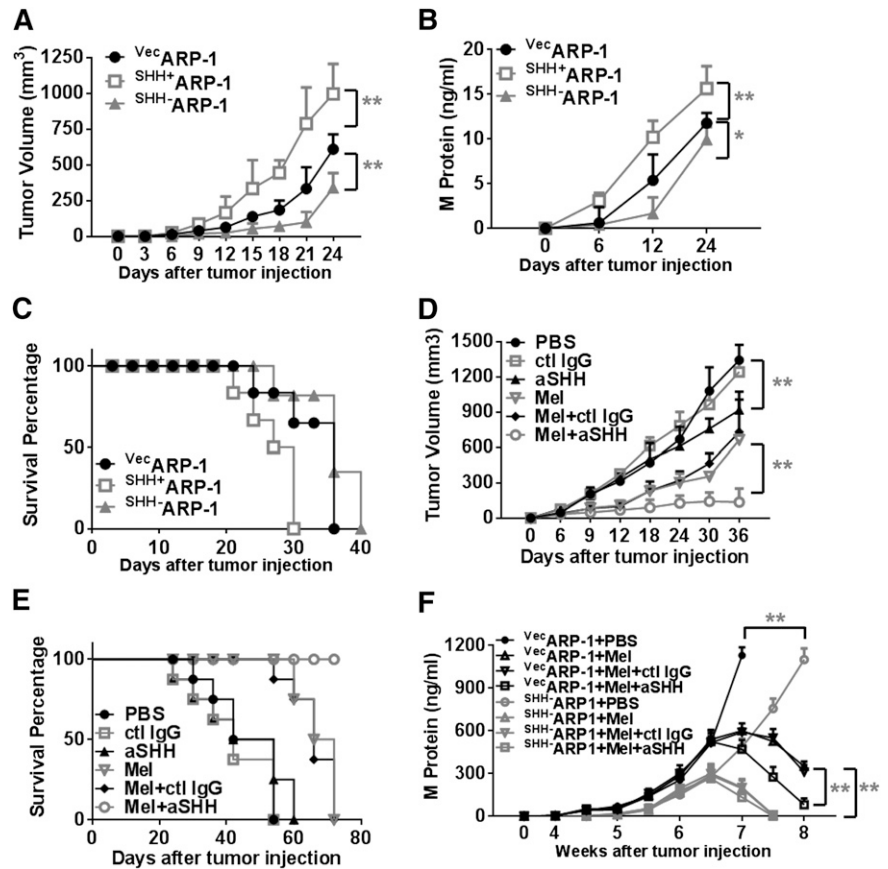
SCID mice, and 4 weeks later, we injected  $1 \times 10^6$  <sup>vec</sup>ARP-1 or <sup>SHH</sup>-ARP-1 cells into the fetal bone cavities to mimic MM infiltration in the human BM microenvironment. After MM was established, we intraperitoneally injected Mel (50 μg per mouse) or equal amounts of PBS, together with or without anti-SHH antibody or control IgG (intrabone injection) every 3 days. Tumor burdens were monitored by measuring the levels of circulating human M-protein (human IgG) every week. Our results showed that, compared with control cells, MM cells with SHH knocked down grew significantly more slowly (<sup>vec</sup>ARP-1 + PBS vs <sup>SHH</sup>-ARP-1 + PBS groups; *P* < .001; Figure 7F). In mice injected with control MM cells, treatment with Mel dramatically reduced tumor burden, and injection of anti-SHH antibody further retarded tumor growth (<sup>vec</sup>ARP-1 + Mel + control IgG vs <sup>vec</sup>ARP-1 + Mel + αSHH groups; *P* < .001; Figure 7F). However, in mice injected with <sup>SHH</sup>-ARP-1 MM cells, treatment with Mel also dramatically reduced tumor burden, but injection of anti-SHH antibody had no additive antimyeloma effect (<sup>SHH</sup>-ARP-1 + Mel + control IgG vs <sup>SHH</sup>-ARP-1 + Mel + αSHH groups; *P* > .05; Figure 7F). Thus, these results strongly suggest that MM-derived SHH, but not BM stroma-derived SHH, plays a key role in MM cell growth and drug resistance in vivo.

## Discussion

Our study elucidates a novel mechanism of Hh signaling in MM chemotherapy resistance and evaluates the Hh signaling as a novel



**Figure 7. MM-derived autocrine SHH promotes MM cell growth and drug resistance in vivo.** Shown are tumor burdens detected as (A) tumor volumes or (B) levels of M-protein secreted by human MM cells (<sup>vec</sup>ARP-1, <sup>SHH+</sup>ARP-1, or <sup>SHH-</sup>ARP-1 cells) in SCID mice, and (C) survival of the mice. In this experiment, 2 × 10<sup>5</sup> MM cells were injected into SCID mice subcutaneously. Tumor volume (in cubic millimeters) was measured every 3 days, and the levels of circulating M-protein were detected weekly by ELISA. Also shown are (D) tumor volumes and (E) survival of ARP-1-inoculated mice treated with Mel in combination with aSHH. Injection of PBS, control IgG, aSHH, or Mel alone served as controls. In these experiments, when subcutaneous tumors reached 5 mm in diameter, mice were treated with intraperitoneal injections of Mel (50 μg per mouse every 3 days for the duration of the experiment) or 50 μL PBS, with or without aSHH or control IgG (5 μg per mouse every 3 days for the duration of the experiment) injected around the tumor. Mice were euthanized when they became moribund or when subcutaneous tumors reached 15 mm in diameter. (F) Levels of M-protein secreted by <sup>vec</sup>ARP-1- or <sup>SHH+</sup>ARP-1-inoculated SCID-hu mice treated with Mel in combination with aSHH. Injection of PBS, control IgG, aSHH, or Mel alone served as controls. \*P < .05; \*\*P < .01.



therapeutic target in MM. First, we demonstrated that autocrine expression in MM cells, but not paracrine expression in MSCs, is a major source of SHH within BM. Second, we demonstrated that patients' CD138<sup>+</sup>CD19<sup>-</sup> primary MM cells and MM cell lines, but not CD138<sup>-</sup>CD19<sup>+</sup> cancer stem cells, expressed and secreted SHH. Finally, MM-derived SHH activated Hh signaling and upregulated BCL-2 expression in MM cells, leading to protection of MM cells from chemotherapy-induced apoptosis. Recently, a new drug called vismodegib, which inhibits Hh signaling, has been evaluated in several malignancies including MM, and it has been approved by the US Food and Drug Administration's priority review program for the treatment of advanced basal-cell carcinoma.<sup>28</sup> Therefore, knowledge obtained from our study could potentially facilitate the fine-tuning of clinical studies that use Hh signaling inhibitors in MM patients.

A previous study reported that malignant cells from patients with MM and non-Hodgkin lymphoma and from a transgenic mouse model of B-cell lymphoma all responded to cyclopamine treatment by growth inhibition in vitro, and Hh pathway inhibition in vivo had a positive effect on the survival of mice.<sup>13</sup> They further concluded that stromally produced SHH plays an essential role in supporting malignant plasma cell survival based on the data that BM-derived, in vitro cultured stromal cells and/or MSCs produced high amounts of SHH that supported myeloma cell survival. However, myeloma cells cultured in vitro with a feeder layer of MSCs is quite different from primary MM cells in the actual BM environment, because the frequency of MSCs in BM mononuclear cell fraction from humans is only 1 in 1 × 10<sup>5</sup> to 1 × 10<sup>6</sup> cells.<sup>29,30</sup> In line with these results, when we used CD90 and CD166 markers to detect MSCs in normal and MM patients' BM samples, the numbers of MSCs in BM samples

were extremely low. Therefore, cultured BM-derived MSCs, although producing high amounts of SHH in vitro but being very low in number in the BM, cannot provide sufficient SHH for MM cells in situ, and these cells cannot truly represent BM stromal cells in MM patients. Indeed, when we examined the cells that expressed and secreted SHH in MM patients' BM aspirate or biopsy samples, our data uniformly showed that CD138<sup>+</sup> MM plasma cells, but not other cells in the BM, are the major contributor of the protein. Our in vivo studies using the MM mouse model, especially the MM-SCID-hu mouse model in which human BM microenvironment was present, further excluded the possibility that stroma-derived SHH plays a crucial role in MM pathogenesis. Thus, we conclude that, based on our results, MM-derived autocrine SHH plays a crucial role in MM survival and induction of drug resistance. Our study does not, however, exclude the possibility that paracrine SHH from BM stromal cells may also play a minor role in MM pathogenesis.

Peacock et al<sup>14</sup> found that Hh pathway activity was manifested within the CD138<sup>-</sup>CD19<sup>+</sup> tumor stem cell but not in the CD19<sup>-</sup>CD138<sup>+</sup> MM plasma cell compartments, and stroma-derived Hh ligand maintained a tumor stem cell compartment in MM. In our study, we carefully examined whether highly purified CD138<sup>+</sup> MM plasma cells expressed Hh signaling components and responded to SHH stimulation. Our results showed that the SHH ligand, the ligand receptor PTCH, and the transcription factor GLI1 were all commonly expressed in both CD138<sup>+</sup> primary MM cells from patients and MM cell lines, and the SHH/GLI1 signaling pathway played an important role in CD138<sup>+</sup> MM cell survival and chemotherapy resistance in vitro and in vivo. Thus, we believe that CD138<sup>+</sup> MM plasma cells not only are the major producer of SHH but also are the major downstream target cells of Hh signaling. Because the reasons for the

discrepancy between these two studies are not obvious, further studies may be needed to address this issue.

So far, 3 models have been proposed for explaining aberrant Hh signaling activity in development and/or oncogenesis: (1) ligand-independent signaling, (2) ligand-dependent autocrine/juxtacrine signaling, and (3) ligand-dependent paracrine signaling.<sup>8</sup> Bushman and colleagues were the first to propose the paracrine manner of SHH signaling in the stromal cells in prostate cancer.<sup>31</sup> Thereafter, several other publications confirmed this type of Hh secretion in the development and differentiation of MM and other tumors.<sup>32-36</sup> Additionally, the biological functions of autocrine Hh signaling have also been demonstrated in morphogenesis, pathophysiologic processes, and tumorigenesis.<sup>37-40</sup> However, autocrine Hh signaling in tumors was demonstrated in experiments that showed the inhibition of tumor growth via the Hh ligand-neutralizing antibody,<sup>41,42</sup> treatment with cyclopamine,<sup>43</sup> or RNA interference-mediated knockdown of SMO or GLI1.<sup>44</sup> Autocrine Hh ligand has not directly been shown to activate the Hh signaling pathway. In our study, data showed that autocrine SHH in the CD138<sup>+</sup> cells promoted MM tumorigenesis and drug resistance. In line with our results, Blotta et al<sup>28</sup> showed that SHH was expressed in the CD138<sup>+</sup> population and that Hh signaling played a significant role in the growth and survival of MM cells. Agarwal et al<sup>45</sup> also showed that inhibition of Hh signaling by activation of the liver X receptors suppressed MM cell clonogenic growth and self-renewal both in vitro and in vivo.<sup>28,45</sup>

In conclusion, we showed that autocrine SHH signaling, rather than paracrine SHH signaling, protects MM cells from apoptosis, promotes MM cell proliferation in vitro and in vivo, and enhances MM drug resistance in vitro and in vivo. We also explored the molecular mechanism by which autocrine SHH signaling influences MM cell survival and chemotherapy resistance. Hh signaling has been reported to induce the resistance of myeloid leukemia cells to multiple drugs,<sup>46</sup> and mechanisms that include the regulation of the expression levels of antiapoptotic molecules or ATP-binding cassettes and MDR family members have been reported.<sup>47</sup> However,

we did not find any changes in the mRNA expression of MDR1, MDR2, MDR3, AP1, or TAP2. Our data suggest that autocrine SHH-induced chemotherapy resistance in MM cells may be mediated by its downstream target BCL-2.

## Acknowledgments

The authors thank the Departmental Myeloma Tissue Bank for patient samples.

This work was supported by National Cancer Institute grants R01s CA138402, CA138398, CA163881, and P50 CA142509 (Q.Y.), Leukemia and Lymphoma Society Translational Research grants (Q.Y.), and National Cancer Institute grant K99/R00 CA137158 (J.Y.).

## Authorship

Contribution: Z.L., J.Y., and Q.Y. initiated the work, designed the experiments, and wrote the paper; Z.L., J.X., J.H., Y.Z., H.L., Y.L., P.L., and J.Q. performed the experiments and statistical analyses; and P.L. and D.M.W. provided samples and critical suggestions for this study.

Conflict-of-interest disclosure: The authors declare no competing financial interests.

The current affiliation for Y.Z., H.L., Y.L., J.Q., and Q.Y. is Department of Cancer Biology, Lerner Research Institute, Cleveland Clinic, Cleveland, OH.

Correspondence: Qing Yi, Department of Cancer Biology, Lerner Research Institute, Cleveland Clinic, 9500 Euclid Ave, NB40, Cleveland, OH 44195; e-mail: yiq@ccf.org; and Jing Yang, Department of Lymphoma and Myeloma, Unit 903, The University of Texas MD Anderson Cancer Center, 1515 Holcombe Blvd, Houston, TX 77030; e-mail: jiyang@mdanderson.org.

## References

- Kyle RA, Rajkumar SV. Multiple myeloma. *N Engl J Med*. 2004;351(18):1860-1873.
- Palumbo A, Anderson K. Multiple myeloma. *N Engl J Med*. 2011;364(11):1046-1060.
- Brenner H, Gondos A, Pulte D. Recent major improvement in long-term survival of younger patients with multiple myeloma. *Blood*. 2008; 111(5):2521-2526.
- Wetmore C. Sonic hedgehog in normal and neoplastic proliferation: insight gained from human tumors and animal models. *Curr Opin Genet Dev*. 2003;13(1):34-42.
- Varjosalo M, Taipale J. Hedgehog: functions and mechanisms. *Genes Dev*. 2008;22(18): 2454-2472.
- Marigo V, Tabin CJ. Regulation of patched by sonic hedgehog in the developing neural tube. *Proc Natl Acad Sci USA*. 1996;93(18):9346-9351.
- Duman-Scheel M, Weng L, Xin S, Du W. Hedgehog regulates cell growth and proliferation by inducing Cyclin D and Cyclin E. *Nature*. 2002; 417(6886):299-304.
- Teglund S, Toftgård R. Hedgehog beyond medulloblastoma and basal cell carcinoma. *Biochim Biophys Acta*. 2010;1805(2):181-208.
- Lindemann RK. Stroma-initiated hedgehog signaling takes center stage in B-cell lymphoma. *Cancer Res*. 2008;68(4):961-964.
- Kim JE, Singh RR, Cho-Vega JH, et al. Sonic hedgehog signaling proteins and ATP-binding cassette G2 are aberrantly expressed in diffuse large B-cell lymphoma. *Mod Pathol*. 2009;22(10): 1312-1320.
- Tam M, Lin P, Hu P, Lennon PA. Examining Hedgehog pathway genes GLI3, SHH, and PTCH1 and the p53 target GLIPR1/GLIPR1L1/GLIPR1L2 gene cluster using fluorescence in situ hybridization uncovers GLIPR1/GLIPR1L1/GLIPR1L2 deletion in 9% of patients with multiple myeloma. *J Assoc Genet Technol*. 2010;36(3): 111-114.
- Katoh Y, Katoh M. Hedgehog target genes: mechanisms of carcinogenesis induced by aberrant hedgehog signaling activation. *Curr Mol Med*. 2009;9(7):873-886.
- Dierks C, Grbic J, Zirikli K, et al. Essential role of stromally induced hedgehog signaling in B-cell malignancies. *Nat Med*. 2007;13(8):944-951.
- Peacock CD, Wang Q, Gesell GS, et al. Hedgehog signaling maintains a tumor stem cell compartment in multiple myeloma. *Proc Natl Acad Sci USA*. 2007;104(10):4048-4053.
- He J, Liu Z, Zheng Y, et al. p38 MAPK in myeloma cells regulates osteoclast and osteoblast activity and induces bone destruction. *Cancer Res*. 2012;72(24):6393-6402.
- Li T, Liu Z, Hu X, Ma K, Zhou C. Involvement of ERK-RSK cascade in phenylephrine-induced phosphorylation of GATA4. *Biochim Biophys Acta*. 2012;1823(2):582-592.
- Yang J, Zhang X, Wang J, et al. Anti beta2-microglobulin monoclonal antibodies induce apoptosis in myeloma cells by recruiting MHC class I to and excluding growth and survival cytokine receptors from lipid rafts. *Blood*. 2007; 110(8):3028-3035.
- Yaccoby S, Barlogie B, Epstein J. Primary myeloma cells growing in SCID-hu mice: a model for studying the biology and treatment of myeloma and its manifestations. *Blood*. 1998;92(8): 2908-2913.
- Compendia Bioscience. Oncomine. Available at: www.oncomine.org. Accessed October 12, 2012.
- Ge S, Mrozik KM, Menicanin D, Gronthos S, Bartold PM. Isolation and characterization of mesenchymal stem cell-like cells from healthy and inflamed gingival tissue: potential use for clinical therapy. *Regen Med*. 2012;7(6):819-832.
- Mödder UI, Roforth MM, Nicks KM, et al. Characterization of mesenchymal progenitor cells isolated from human bone marrow by negative selection. *Bone*. 2012;50(3):804-810.
- Tukachinsky H, Kuzmickas RP, Jao CY, Liu J, Salic A. Dispatched and scube mediate the efficient secretion of the cholesterol-modified

- hedgehog ligand. *Cell Reports*. 2012;2(2):308-320.
23. Taipale J, Chen JK, Cooper MK, et al. Effects of oncogenic mutations in Smoothened and Patched can be reversed by cyclopamine. *Nature*. 2000;406(6799):1005-1009.
  24. Cooper MK, Porter JA, Young KE, Beachy PA. Teratogen-mediated inhibition of target tissue response to Shh signaling. *Science*. 1998;280(5369):1603-1607.
  25. Chen M, Guerrero AD, Huang L, et al. Caspase-9-induced mitochondrial disruption through cleavage of anti-apoptotic BCL-2 family members. *J Biol Chem*. 2007;282(46):33888-33895.
  26. Yang J, Qian J, Wezeman M, et al. Targeting beta2-microglobulin for induction of tumor apoptosis in human hematological malignancies. *Cancer Cell*. 2006;10(4):295-307.
  27. Yang J, Wezeman M, Zhang X, et al. Human C-reactive protein binds activating Fcγ receptors and protects myeloma tumor cells from apoptosis. *Cancer Cell*. 2007;12(3):252-265.
  28. Blotta S, Jakubikova J, Calimeri T, et al. Canonical and noncanonical Hedgehog pathway in the pathogenesis of multiple myeloma. *Blood*. 2012;120(25):5002-5013.
  29. Martin DR, Cox NR, Hathcock TL, Niemeyer GP, Baker HJ. Isolation and characterization of multipotential mesenchymal stem cells from feline bone marrow. *Exp Hematol*. 2002;30(8):879-886.
  30. Haynesworth SE, Goshima J, Goldberg VM, Caplan AL. Characterization of cells with osteogenic potential from human marrow. *Bone*. 1992;13(1):81-88.
  31. Fan L, Pepicelli CV, Dibble CC, et al. Hedgehog signaling promotes prostate xenograft tumor growth. *Endocrinology*. 2004;145(8):3961-3970.
  32. Outram SV, Varas A, Pepicelli CV, Crompton T. Hedgehog signaling regulates differentiation from double-negative to double-positive thymocyte. *Immunity*. 2000;13(2):187-197.
  33. James AW, Levi B, Commons GW, Glotzbach J, Longaker MT. Paracrine interaction between adipose-derived stromal cells and cranial suture-derived mesenchymal cells. *Plast Reconstr Surg*. 2010;126(3):806-821.
  34. Kolterud A, Grosse AS, Zacharias WJ, et al. Paracrine Hedgehog signaling in stomach and intestine: new roles for hedgehog in gastrointestinal patterning. *Gastroenterology*. 2009;137(2):618-628.
  35. Lin N, Tang Z, Deng M, et al. Hedgehog-mediated paracrine interaction between hepatic stellate cells and marrow-derived mesenchymal stem cells. *Biochem Biophys Res Commun*. 2008;372(1):260-265.
  36. Liu Z, Li T, Reinhold MI, Naski MC. MEK1-RSK2 contributes to Hedgehog signaling by stabilizing GLI2 transcription factor and inhibiting ubiquitination. *Oncogene*. 2014;33(1):65-73.
  37. Chen YJ, Lin CP, Hsu ML, Shieh HR, Chao NK, Chao KS. Sonic hedgehog signaling protects human hepatocellular carcinoma cells against ionizing radiation in an autocrine manner. *Int J Radiat Oncol Biol Phys*. 2011;80(3):851-859.
  38. Handrigan GR, Richman JM. Autocrine and paracrine Shh signaling are necessary for tooth morphogenesis, but not tooth replacement in snakes and lizards (Squamata). *Dev Biol*. 2010;337(1):171-186.
  39. Varas A, Hernández-López C, Valencia J, et al. Survival and function of human thymic dendritic cells are dependent on autocrine Hedgehog signaling. *J Leukoc Biol*. 2008;83(6):1476-1483.
  40. Zhou X, Liu Z, Jang F, Xiang C, Li Y, He Y. Autocrine Sonic hedgehog attenuates inflammation in cerulein-induced acute pancreatitis in mice via upregulation of IL-10. *PLoS ONE*. 2012;7(8):e44121.
  41. Berman DM, Karhadkar SS, Maitra A, et al. Widespread requirement for Hedgehog ligand stimulation in growth of digestive tract tumours. *Nature*. 2003;425(6960):846-851.
  42. Sanchez P, Hernández AM, Stecca B, et al. Inhibition of prostate cancer proliferation by interference with SONIC HEDGEHOG-GLI1 signaling. *Proc Natl Acad Sci USA*. 2004;101(34):12561-12566.
  43. Zhao C, Chen A, Jamieson CH, et al. Hedgehog signalling is essential for maintenance of cancer stem cells in myeloid leukaemia. *Nature*. 2009;458(7239):776-779.
  44. Yuan Z, Goetz JA, Singh S, et al. Frequent requirement of hedgehog signaling in non-small cell lung carcinoma. *Oncogene*. 2007;26(7):1046-1055.
  45. Agarwal JR, Wang Q, Tanno T, et al. Activation of liver x receptors inhibits hedgehog signaling, clonogenic growth, and self-renewal in multiple myeloma. *Mol Cancer Ther*. 2014;13(7):1873-1881.
  46. Queiroz KC, Ruela-de-Sousa RR, Fuhler GM, et al. Hedgehog signaling maintains chemoresistance in myeloid leukemic cells. *Oncogene*. 2010;29(48):6314-6322.
  47. Sims-Mourtada J, Izzo JG, Ajani J, Chao KS. Sonic Hedgehog promotes multiple drug resistance by regulation of drug transport. *Oncogene*. 2007;26(38):5674-5679.